Metabolic labeling and direct imaging of choline phospholipids in vivo

Cindy Y. Jao[a], Mary Roth[b], Ruth Welti[b], and Adrian Salic[a,1]

[a]Department of Cell Biology, Harvard Medical School, 240 Longwood Avenue, Boston, MA 02115; and [b]Kansas Lipidomics Research Center, Division of Biology, Kansas State University, Manhattan, KS 66506

Communicated by Howard Green, Harvard Medical School, Boston, MA, July 16, 2009 (received for review March 4, 2009)

Choline (Cho)-containing phospholipids are the most abundant phospholipids in cellular membranes and play fundamental structural as well as regulatory roles in cell metabolism and signaling. Although much is known about the biochemistry and metabolism of Cho phospholipids, their cell biology has remained obscure, due to the lack of methods for their direct microscopic visualization in cells. We developed a simple and robust method to label Cho phospholipids in vivo, based on the metabolic incorporation of the Cho analog propargylcholine (propargyl-Cho) into phospholipids. The resulting propargyl-labeled phospholipid molecules can be visualized with high sensitivity and spatial resolution in cells via a Cu(I)-catalyzed cycloaddition reaction between the terminal alkyne group of propargyl-Cho and a labeled azide. Total lipid analysis of labeled cells shows strong incorporation of propargyl-Cho into all classes of Cho phospholipids; furthermore, the fatty acid composition of propargyl-Cho-labeled phospholipids is very similar to that of normal Cho phospholipids. We demonstrate the use of propargyl-Cho in cultured cells, by imaging phospholipid synthesis, turnover, and subcellular localization by both fluorescence and electron microscopy. Finally, we use propargyl-Cho to assay microscopically phospholipid synthesis in vivo in mouse tissues.

alkyne | azide | click chemistry | membrane | microscopy

Phospholipids are the major components of all cellular membranes. The most common phospholipid head group in eukaryotes is choline (Cho) (1). Cho-containing phospholipids are important structural components of membranes and play critical roles in cell signaling, either as signaling molecules in their own right or as precursors of secondary messengers.

Cho phospholipids include phosphatidylcholine (PC), sphingomyelin (SM), and ether phospholipids with a Cho head group (ePC). PC is the most abundant phospholipid in most eukaryotic cells, comprising almost 50% of the phospholipid pool. SM is an important component of myelin sheaths, making up 10% of brain phospholipids. Ether PCs are less abundant, except in white blood cells, in which they reach half the level of PC (2), and are precursors of the platelet-activating factor, a phospholipid with potent inflammatory activity.

Cho enters cells through specific membrane transporters, is phosphorylated by Cho kinase, and is usually activated as CDP-Cho (3). In PC biosynthesis, Cho is transferred from CDP-Cho to diacylglycerol, in the endoplasmic reticulum. In the case of SM, the Cho head group is transferred from PC to ceramide, in the Golgi. How ePC molecules acquire Cho head groups is still obscure (2).

Despite a wealth of knowledge about the metabolism of Cho phospholipids, their cell biology is poorly understood. We still do not understand how Cho phospholipid synthesis is regulated in cells, how they are transported between organelles, how they move between the leaflets of membrane bilayers, or how they take part in the organization of membrane microdomains. Deciphering the cell biology of Cho phospholipids would be greatly aided by having the ability to metabolically label them followed by high-resolution microscopic imaging.

We took advantage of the pathway for cellular Cho utilization to develop a method to visualize Cho phospholipids. We synthesized the Cho analog propargylcholine (propargyl-Cho), which bears a terminal alkyne moiety, and incorporates efficiently into all classes of Cho phospholipids in cultured cells, replacing half or more of the Cho head groups in total lipids after 24 h. Propargyl-Cho also incorporates strongly into phospholipids in whole animals. Propargyl-Cho-labeled phospholipids can be revealed for light or for electron microscopy by covalent attachment of a labeled azide, via a Cu(I)-catalyzed [3 + 2] reaction (“click” chemistry) (4, 5). This strategy to label and detect Cho phospholipids in vivo should allow their direct visualization in cells and tissues and facilitate investigations of their cell biology.

Metabolic incorporation of labeled precursors, followed by chemical derivatization has been used for microscopic visualization in cells of macromolecules such as glycoproteins [labeled with sugar analogs (6, 7)], proteins [labeled with amino acid analogs (8, 9)], and DNA (10) and RNA (11) (labeled with nucleoside analogs). The present study uses this strategy to biosynthetically label and microscopically image a small molecule cellular component—a complex lipid.

Results and Discussion

Labeling Cells with Propargylcholine, a Choline Analog. Studies of Cho requirement in insect development demonstrated that Cho analogs in which a methyl group is replaced with an alkyl chain up to five carbons in length incorporate efficiently into phospholipids (12–14). We reasoned that propargylcholine (propargyl-Cho) (Fig. 1*A*), in which one methyl is replaced by a three-carbon propargyl group will likewise be used by cells in place of Cho, as a phospholipid precursor. The resulting phospholipids could then be detected with a labeled azide using a Cu(I)-catalyzed [3 + 2] cycloaddition. We synthesized propargyl-Cho and tested its incorporation into NIH 3T3 cells. Cells incubated with propargyl-Cho for 24 h, then fixed and stained with Alexa568-azide, showed strong staining proportional in intensity to the concentration of added propargyl-Cho (Fig. 1*B*). Other fluorescent azides [such as the aromatic fluorescein-azide (10)], also stain propargyl-Cho-labeled cells efficiently (Figs. 1*D* and 4*A*). Propargyl-Cho staining was very intense and mostly uniform across the cell population, with small cell-to-cell differences. The propargyl-Cho stain localized to cellular membranes, a pattern consistent with incorporation into phospholipids.

Two results suggest that propargyl-Cho incorporates into phospholipids. First, the staining is very sensitive to detergents, consistent with the fact that propargyl-Cho phospholipids are not covalently attached to the fixed cells (Fig. S1). Second,

Author contributions: C.Y.J. and A.S. designed research; C.Y.J., M.R., R.W., and A.S. performed research; M.R. and R.W. contributed new reagents/analytic tools; C.Y.J., M.R., R.W., and A.S. analyzed data; and C.Y.J., R.W., and A.S. wrote the paper.

The authors declare no conflict of interest.

[1]To whom correspondence should be addressed. E-mail: asalic@hms.harvard.edu.

This article contains supporting information online at www.pnas.org/cgi/content/full/0907864106/DCSupplemental.

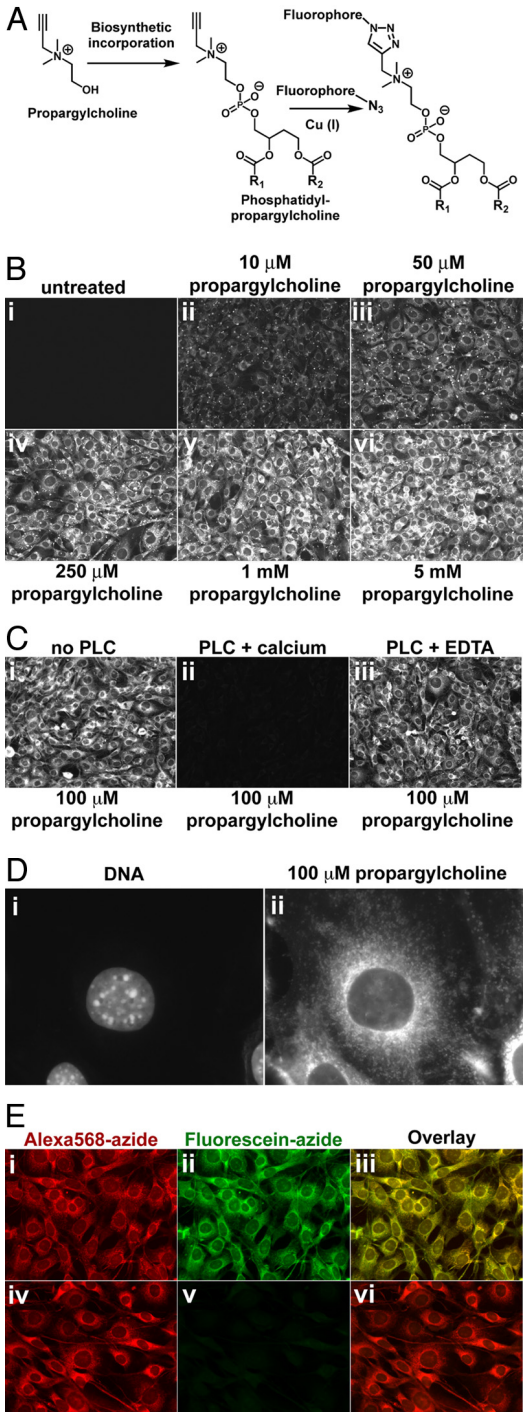

Fig. 1. Imaging choline-containing phospholipids in cells with propargylcholine. (*A*) Propargyl-Cho, a biosynthetic label for Cho phospholipids. Phospholipid molecules bearing a terminal alkyne group can be detected by ''click'' chemistry using a fluorescent azide. (*B*) Propargyl-Cho incorporation into NIH 3T3 cells. Cells labeled overnight with varying concentrations of propargyl-Cho were fixed and stained with Alexa568-azide. Note the low background in the absence of propargyl-Cho (*i*) and the increase in staining intensity with increasing propargyl-Cho concentration (*ii–vi*). (*C*) Treatment of fixed cells with phospholipase C, which removes Cho head groups of phospholipids, strongly decreases propargyl-Cho staining by Alexa568-azide (compare *ii* to *i*). Phospholipase C requires calcium for activity; in the absence of calcium, propargyl-Cho staining is not affected by phospholipase C (*iii*). (*D*) Higher magnification fluorescence micrograph showing propargyl-Cho labeling of cellular organelles. (*E*) Reproducibility of propargyl-Cho staining. Cells labeled with 100 μM propargyl-Cho overnight were stained with 10 μM Alexa568-azide (*i*) and then with 20 μM fluorescein-azide (*ii*). Strong red and green signals indicate that the first staining reaction does not consume the incorporated propargyl-Cho. The red and green staining patterns are identical (*iii*), indicating that the two successive reactions detect the same phospholipid populations. The propargyl-Cho label can be consumed if, after Alexa568-azide (*iv*), cells are reacted with 5 mM non-fluorescent azide; this abolishes staining with fluorescein-azide (*v* and *vi*).

incubation of fixed, propargyl-Cho-labeled cells with phospholipase C (PLC, which hydrolyzes Cho head groups to Cho phosphate) abolishes propargyl-Cho staining (Fig. 1*C*).

Higher magnification fluorescence micrographs (Fig. 1*D*) show that propargyl-Cho incorporates into a large number of intracellular structures, including ones that are vesicular, tubular and reticular in shape. The plasma membrane stains strongly, although the signal is significantly smaller than that of intracellular membranes. The stain is excluded from the nucleus. It should be noted that all cultured cells used in this study were grown in complete media, which contains 30 μM Cho. Propargyl-Cho can thus compete effectively with Cho for incorporation into phospholipids.

Only a fraction of the incorporated propargyl-Cho reacts with Alexa568-azide at the concentration used in our experiments (Fig. 1*E*). If propargyl-Cho-labeled cells are stained with Alexa568-azide and then with fluorescein-azide, both the red (Fig. 1*Ei*) and the green (Fig. 1*Eii*) signals are strong. Importantly, the staining patterns of fluorescein-azide and Alexa568-azide are identical, demonstrating the reproducibility of propargyl-Cho detection (Fig. 1*Eiii*). The propargyl-Cho left unreacted with Alexa568-azide can be completely reacted using a higher concentration of the non-fluorescent azide, O-(2-aminoethyl)-O'-(2-azidoethyl)-pentaethylene glycol (Fig. 1*Eiv–vi*).

Cells labeled with 500 μM propargyl-Cho for 48 h showed no obvious toxicity and continued dividing during incubation, indicating that propargyl-Cho is well tolerated even at high concentrations. Furthermore, cells labeled with 250 μM propargyl-Cho for 24 h, then washed and grown for over one week did not show signs of toxicity, while maintaining high levels of incorporated propargyl-Cho.

Propargylcholine Incorporates into Cellular Lipids with High Efficiency. We determined the effect of propargyl-Cho labeling on cellular lipids and measured its incorporation into cellular phospholipids by electrospray ionization-tandem mass spectrometry (ESI-MS/MS) analysis of total lipids isolated from NIH 3T3 cells labeled for 24 h with 0, 100, 250, or 500 μM propargyl-Cho (Fig. 2 and Figs. S2–S8). Propargyl-Cho labeling does not significantly affect the relative abundance of non-Cho phospholipids (Fig. 2*A*)—for example, PE constitutes 53%, 53%, 55%, and 51% of the total non-Cho phospholipids in cells labeled with 0, 100, 250, and 500 μM propargyl-Cho, respectively. Labeling cells with propargyl-Cho thus does not cause an obvious alteration in the metabolism of non-Cho phospholipids.

Propargyl-Cho incorporates efficiently into all Cho phospholipid classes (Fig. 2*B* and Fig. S2), proportional to the concentration of added propargyl-Cho. In total PC phospholipids, 18%, 33%, and 44% of Cho is replaced by propargyl-Cho after labeling with 100, 250, and 500 μM propargyl-Cho. These numbers are in good accord with our measurements of propargyl-Cho incorporation by phospholipase D hydrolysis and mass spectrometry (Fig. S9). Interestingly, after 24 h, the incorporation of propargyl-Cho is lower for SM (5% at 100 μM, 10% at 250 μM, and 15% at 500 μM propargyl-Cho) than for PC. We speculate that this difference is due to the slower equilibration of propargyl-Cho into the SM pool, consistent with the fact that SM biosynthesis requires the transfer of Cho from previously formed PC molecules. Propargyl-Cho also equilibrates slower into the ePC

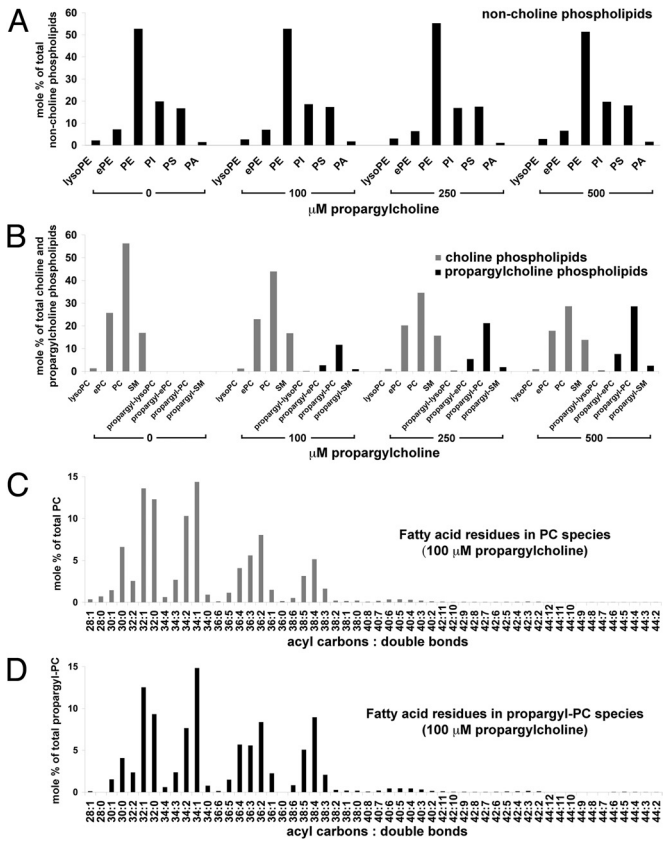

Fig. 2. Total lipid analysis of propargylcholine-labeled cells. Total lipids isolated from NIH 3T3 cells labeled for 24 h with 0, 100, 250, and 500 μM propargyl-Cho were quantified by electrospray ionization-tandem mass spectrometry. Amounts of various phospholipids are shown as mole percentages of total non-Cho phospholipids (*A*), total Cho and propargyl-Cho phospholipids (*B*), total PC species (*C*), and total propargyl-PC species (*D*). (*A*) Distribution of non-Cho phospholipids (lyso-phosphatidylethanolamine, lyso-PE; ether-linked phosphatidylethanolamine, ePE; phosphatidylethanolamine, PE; phosphatidylinositol, PI; phosphatidylserine, PS; phosphatidic acid, PA) in cells labeled with propargyl-Cho. Propargyl-Cho labeling does not significantly affect the relative amount of non-Cho phospholipid classes. (*B*) Propargyl-Cho incorporates into all phosphatidylcholine (PC) classes (lysoPC; ether-linked PC, ePC; and PC) and into sphingomyelin (SM), proportional to the concentration of propargyl-Cho added to cells. (*C* and *D*) In NIH 3T3 cells labeled with 100 μM propargyl-Cho overnight, the sum fatty acid composition of PC species (*C*) is very similar to that of propargyl-PC species (*D*). Each PC and propargyl-PC species is identified by two numbers: the first is the sum of acyl carbons, and the second is the sum of double bonds present in the two fatty acid residues of the respective phospholipid species.

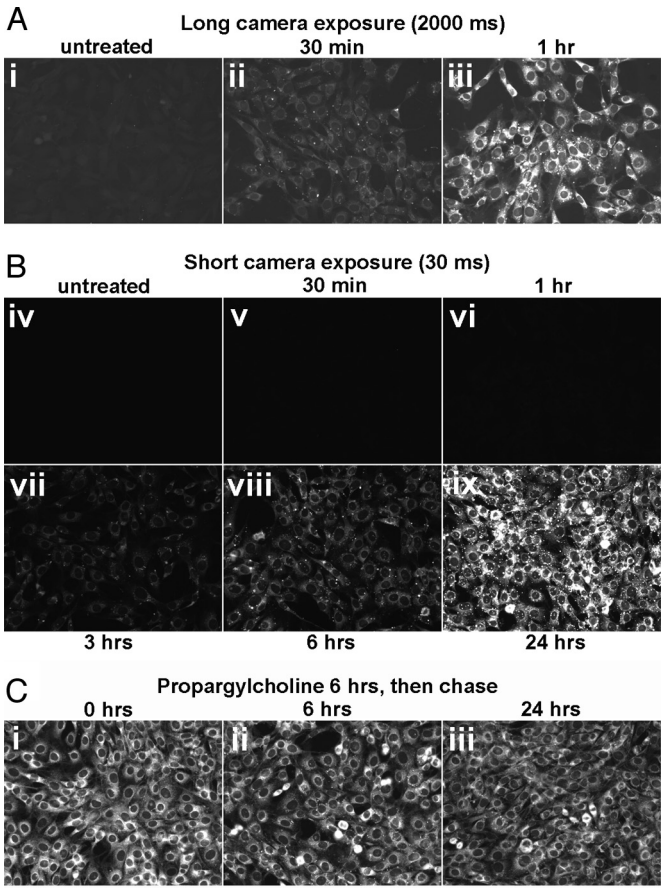

Fig. 3. Rapid synthesis and slow turnover of propargylcholine-labeled phospholipids. (*A*) Time course of propargyl-Cho uptake and incorporation into phospholipids. NIH 3T3 cells were labeled with 1 mM propargyl-Cho in complete media for varying amounts of time and then stained with Alexa568-azide. The propargyl-Cho stain was photographed with a long exposure time (2 s, *i–iii*) or a short exposure time (30 ms, *iv–ix*). Note that propargyl-Cho incorporation is visible 30 min after addition to cells (*ii*) and continues to increase with time (*ii–viii*), saturating after about 24 h (*ix*). (*B*) Stability of propargyl-Cho-labeled phospholipids in cells. NIH 3T3 cells were labeled with 1 mM propargyl-Cho for 6 h and then chased with normal media for different amounts of time (*i–iii*). The intensity of the Alexa568-azide stain does not appreciably decrease after 24 h in culture, indicating the low turnover of propargyl-Cho phospholipids.

pool (Fig. 2*B*), a fact we currently cannot explain due to the poor understanding of how Cho attaches to ePC molecules in cells.

To better characterize propargyl-Cho as a Cho analog, we determined the sum fatty acid composition of each class of phospholipids in NIH 3T3 cells labeled with 0, 100, 250, and 500 μM propargyl-Cho. In the case of non-Cho phospholipids, their sum fatty acid composition was not significantly affected at any of the propargyl-Cho concentrations we tested (Figs. S3–S5), further supporting that propargyl-Cho does not affect the metabolism of non-Cho phospholipids. In the case of Cho phospholipids, the sum fatty acid composition of propargyl-Cho-labeled molecules is very similar to that of the phospholipids carrying a normal Cho head group, at all of the tested propargyl-Cho concentrations (see Fig. 2 *C* and *D* for a comparison between PC and propargyl-PC in cells labeled with 100 μM propargyl-Cho; the complete analysis of the sum fatty acid composition for all classes of Cho phospholipids, at all propargyl-Cho concentrations, is shown in Figs. S6–S8). These results indicate that propargyl-Cho is a good Cho analog, mimicking in detail the properties of Cho in cells.

Kinetics of Propargylcholine Incorporation and of Propargylcholine Phospholipid Turnover in Cells. We asked how long it takes for propargyl-Cho to incorporate into cultured cells. As shown in Fig. 3*A*, the intensity of the propargyl-Cho stain increases gradually with labeling time, reaching very high levels after 24 h. Strong propargyl-Cho labeling is visible after 3–6 h. At longer exposure times, significant propargyl-Cho staining can be detected after labeling for as little as 30 min.

We also determined the stability of propargyl-Cho-labeled phospholipids by pulse-chase. Cells labeled with 1 mM propargyl-Cho for 6 h were washed to remove unincorporated propargyl-Cho and were chased and fixed at different times, followed by azide staining. As shown in Fig. 3*B*, the intensity of the propargyl-Cho stain does not appreciably decrease after 24 h, indicating that propargyl-Cho-labeled phospholipids are stable.

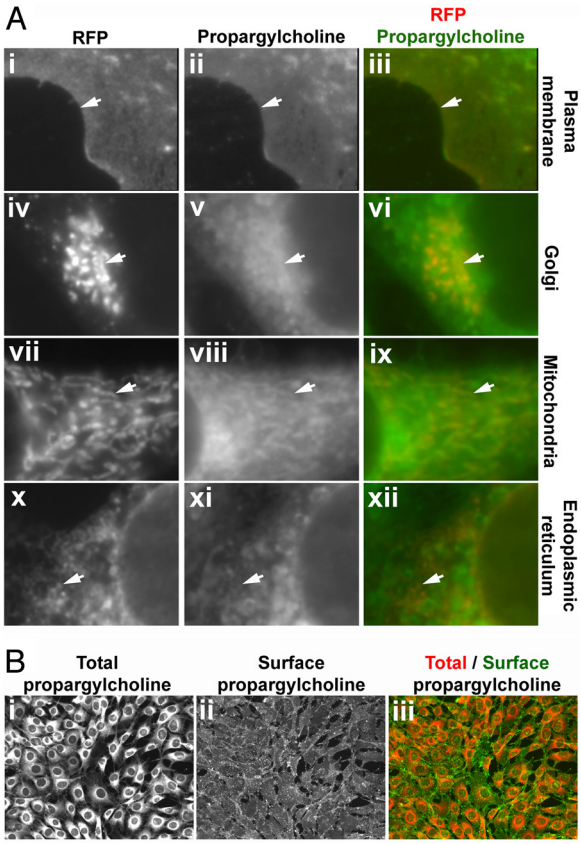

Fig. 4. Subcellular distribution of propargylcholine-labeled phospholipids. (*A*) Co-localization of the propargyl-Cho stain with subcellular markers. Cultured NIH 3T3 cells were transfected with plasmids encoding red fluorescent protein fusions that mark various organelles. The cells were labeled with 100 μM propargyl-Cho overnight and stained with fluorescein-azide. Propargyl-Cho co-localizes with markers for the plasma membrane (*i–iii*), the Golgi (*iv–vi*), mitochondria (*vii–ix*), and endoplasmic reticulum (*x–xii*). The white arrows point to subcellular structures that stain for both propargyl-Cho and a given red fluorescent marker. (*B*) Staining propargyl-Cho phospholipids localized to the outer leaflet of the plasma membrane. Cells labeled with 100 μM propargyl-Cho were reacted with Alexa568-azide and biotin-azide. The latter is visualized specifically on the cell surface by staining with Alexa488-conjugated streptavidin (*ii*), which due to its size does not cross the plasma membrane. The right panel (*iii*) shows the overlay of the total (*i*) and surface (*ii*) propargyl-Cho stain.

This result is consistent with the measured half-life of mammalian phospholipids labeled with radioactive Cho (15, 16) suggesting that propargyl-Cho phospholipid head groups behave similar to Cho in cells.

Distribution of Propargylcholine-Labeled Phospholipids to Cellular Membranes. Cho phospholipids are synthesized primarily in the endoplasmic reticulum (ER) and the Golgi. From these organelles, Cho phospholipids reach other cellular membranes, such as the plasma and mitochondrial membranes. We examined if propargyl-Cho phospholipids populate cellular membranes that contain Cho phospholipids. The plasma membrane, the Golgi, mitochondria and the ER were labeled by expression of specific red fluorescent protein markers (Fig. 4*A*), after which the cells were incubated with 100 μM propargyl-Cho overnight, fixed and stained with fluorescein-azide. As shown in Fig. 4*A*, the propargyl-Cho stain co-localizes with all four subcellular markers, demonstrating that propargyl-Cho-labeled phospholipids, presumably synthesized in the ER and Golgi are subsequently distributed to other cellular membranes.

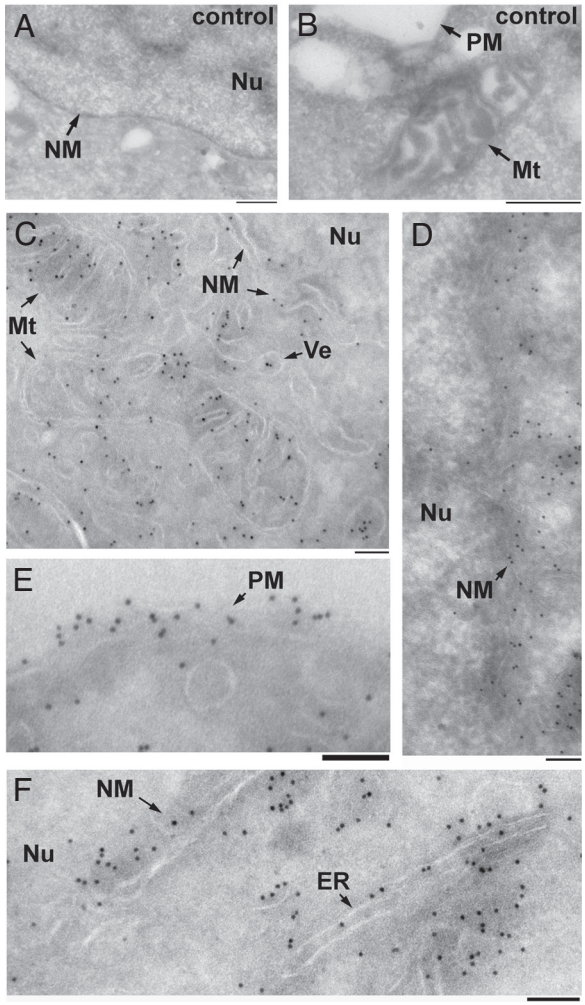

Fig. 5. Visualizing propargylcholine-labeled phospholipids by immuno-electron microscopy of cells. Cultured 293T cells were incubated overnight in the absence (*A* and *B*) or presence (*C–F*) of 100 μM propargyl-Cho, fixed, sectioned on an ultramicrotome and stained with biotin-azide. The sections were then stained with anti-biotin antibodies and protein A-gold (10 nm), counterstained with uranyl acetate and imaged by transmission electron microscopy. Arrows point to various cellular structures: Mt, mitochondria; Nu, nucleus; ER, endoplasmic reticulum; PM, plasma membrane; NM, nuclear membrane; Ve, vesicle. The scale bar in all panels is 100 nm. A negligible number of gold particles are seen on micrographs of control, unlabeled cells (*A* and *B*). Numerous gold particles are seen associated with membranes in cells labeled with propargyl-Cho (*C–F*).

To obtain additional evidence that propargyl-Cho phospholipids reach the plasma membrane, we developed a method to visualize propargyl-Cho on the cell surface. Propargyl-Cho-labeled cells were reacted with both Alexa568-azide and biotin-azide, and biotin was detected with Alexa488-streptavidin. We reasoned that Alexa568-azide penetrates the fixed cells and stains both surface and intracellular phospholipids while Alexa488-streptavidin (molecular weight of 55 kDa) can only access biotin attached to the cell surface. Propargyl-Cho-labeled cells show strong surface labeling with biotin-azide and fluorescent streptavidin staining (Fig. 4*B*), while unlabeled cells show very low background staining. This result demonstrates that propargyl-Cho phospholipids efficiently reach the outer leaflet of the plasma membrane.

Visualization of Propargylcholine-Labeled Phospholipids by Electron Microscopy. We used immuno-electron microscopy to determine precisely what organelles contain propargyl-Cho phospholipids.

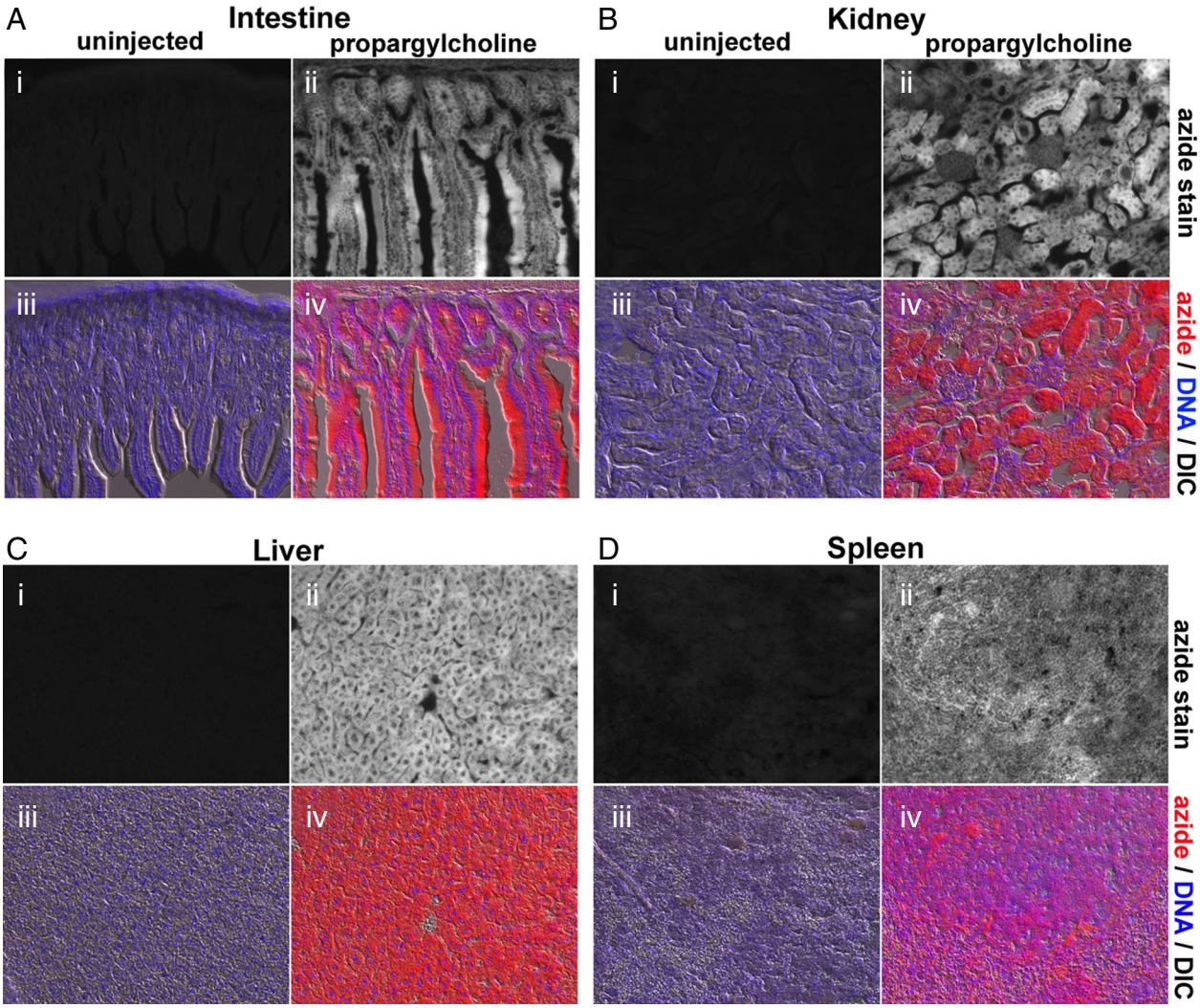

Fig. 6. Imaging the synthesis of choline phospholipids in vivo. Cryostat sections of organs from a propargyl-Cho-injected mouse and from an uninjected control mouse were stained in parallel with TMR-azide. The TMR-azide stain is shown in grayscale (black-and-white images) or in red, overlayed with DNA (blue) and DIC micrographs (color images). Strong propargyl-Cho incorporation is seen in all tissues surveyed: small intestine (*A*), kidney (*B*), liver (*C*), and spleen (*D*).

Cultured 293T cells incubated overnight with or without 100 μM propargyl-Cho were fixed, sectioned frozen on an ultramicrotome and reacted with biotin-azide. Biotin was detected using anti-biotin antibodies and protein A-gold, and the cell sections were negatively stained with uranyl acetate and imaged by transmission electron microscopy. In propargyl-Cho-labeled cells, large numbers of gold particles localize to mitochondria, the plasma membrane, the nuclear membrane, the ER and a large number of vesicles (Fig. 5 *C–F*). Gold particles are largely absent from the nuclei of propargyl-Cho-labeled cells as well as from areas of cytoplasm devoid of membranous structures. Sections through unlabeled cells have little to no gold particles, demonstrating the specificity of the immunogold stain (Fig. 5 *A* and *B*). These experiments further demonstrate that propargyl-Cho labels phospholipids in cellular membranes that normally contain Cho phospholipids. They also represent an instance of direct visualization of Cho phospholipids by electron microscopy in cells.

Metabolic Labeling and Imaging of Choline Phospholipids in Animals. Finally, we wanted to determine if propargyl-Cho could be used to label and image phospholipids in whole animals. One milligram of propargyl-Cho was injected i.p. into a 3-week-old mouse. Organs were harvested and fixed 24 h later, followed by cryostat sectioning and staining with fluorescent azide. As shown in Fig. 6, propargyl-Cho shows very strong labeling of all of the tested mouse tissues. In liver (Fig. 6*C*), the site of abundant phospholipids synthesis, all hepatocytes incorporate propargyl-Cho. Staining is also strong in intestine (Fig. 6*A*), kidney (Fig. 6*B*), and spleen (Fig. 6*D*). Sections from an uninjected control mouse show very low background staining. Our method is thus suitable for visually assaying the synthesis of Cho phospholipids in organs and tissues.

Materials and Methods

Propargyl-Cho Labeling of Cells and Detection by Fluorescence Microscopy. NIH 3T3 cells labeled with propargyl-Cho bromide in complete media (DMEM with 10% bovine calf serum) were fixed with 3.7% formaldehyde in PBS, reacted with 10–20 μM fluorescent azide as described (10), washed with TBS, 0.5 M NaCl, and again TBS. After counterstaining with Hoechst, the cells were imaged by fluorescence microscopy and DIC. To reveal propargyl-Cho labeling of phospholipids on the cell surface, cells labeled with 100 μM propargyl-Cho overnight were fixed with 1% formaldehyde in PBS and then reacted with 10 μM Alexa568-azide and 20 μM biotin-azide. After washing, the cells were incubated with block solution (40 mg/mL BSA in TBS), and stained with 1 μg/mL Alexa488-streptavidin in block solution. The cells were washed with TBS and imaged.

The red fluorescent protein fusions used to determine co-localization with the propargyl-Cho stain were DsRed-Mito (for mitochondria), mCherry-Sec61 (for ER), tdTomato-GalT (for the Golgi), and mCherry-CAAX (for the plasma membrane). Plasmids encoding these constructs were transiently transfected into NIH 3T3 cells, followed by labeling with 100 μM propargyl-Cho overnight. The cells were fixed, stained with 20 μM fluorescein-azide and imaged.

To test phospholipase sensitivity of the propargyl-Cho stain, cells labeled with 100 μM propargyl-Cho overnight were fixed, rinsed with TBS and incubated for 1 h at 37 °C in TBS with 1 mg/mL BSA, in the presence or absence of 0.02 U/mL phospholipase C (PLC type XIV from *C. perfringens*), with 10 mM CaCl2 (required for PLC activity), or 10 mM EDTA (negative control). The cells were washed with TBS and then stained with Alexa568-azide as described above.

To determine the azide concentration required to consume all of the incorporated propargyl-Cho, NIH 3T3 cells were labeled with 100 μM propargyl-Cho overnight, then fixed and stained with 10 μM Alexa568-azide. The cells were washed and incubated for 30 min in staining mixture without fluorescent azide, in the absence or presence of 5 mM O-(2-aminoethyl)-O′-(2-azidoethyl)-pentaethylene glycol (Fluka). The cells were then washed and stained with 20 μM fluorescein-azide.

Mouse Injections. Fifty microliters of a 1M solution of propargyl-Cho in PBS were injected i.p. into a 3-week-old mouse. Tissues were removed 24 h later and fixed in formalin. An uninjected mouse was used as control. The tissues were embedded in OCT medium (Tissue-Tek) and sectioned on a cryostat, followed by staining with 40 μM TMR-azide (10) and Hoechst, as described for cultured cells. The sections were washed extensively with 0.5M NaCl and with TBS, to remove unreacted azide. Extensive washes were required because of the thickness of the cryostat sections compared to a monolayer of cells in culture.

Electron Microscopy. Cultured 293T cells were grown overnight in DMEM supplemented with 10% FBS, with or without 100 μM propargyl-Cho. The cells were washed with PBS, detached from the dish in PBS + 0.5 mM EDTA, pelleted and fixed in 100 mM Na phosphate pH 7.4, 4% formaldehyde (EM Sciences), 0.1% glutaraldehyde (EM Sciences), as described (17). Fixed cell pellets were infiltrated with PBS + 2.3 M sucrose, frozen in liquid nitrogen and sectioned on an ultramicrotome at −120 °C. The 80–100 nm sections were laid on formvar/carbon-coated copper grids for electron microscopy. The grids were stained with biotin-azide as described above for fluorescence microscopy. Biotin was detected using a rabbit anti-biotin antibody (Rockland Immunochemicals), followed by protein A-gold (10-nm colloidal gold). The grids were counterstained and embedded by incubation with 0.3% uranyl acetate in 2% methyl-cellulose (17). The cells were imaged on a Tecnai G2 Spirit BioTWIN transmission electron microscope equipped with an AMT 2k CCD camera.

Lipid Profiling by Electrospray Ionization-Tandem Mass Spectrometry (ESI-MS/MS). Total lipids from cells labeled with various concentrations of propargyl-Cho and from untreated controls were isolated by methanol-chloroform extraction (18), and the solvent was removed under reduced pressure. Lipid analysis by automated ESI-MS/MS, data acquisition, data analysis and acyl group identification were performed as described previously (19, 20), with modifications (*SI Methods*). To determine the absolute amount of various phospholipid classes, the total lipid extract was combined with internal standards, quantified as previously described (21). Phospholipid species containing a given head group were detected from spectra obtained by sequential precursor and neutral loss scans of the total lipid extracts (*SI Methods*).

Chemicals. All chemicals were from Aldrich and were used without further purification. LC/MS analysis was performed on an Agilent 6130 Quadrupole LC/MS instrument. NMR spectra were recorded on a Varian Oxford NMR A5600 (600 MHz) instrument.

TMR-azide, fluorescein-azide and Alexa568-azide were described before (10, 11). Biotin azide was synthesized by reacting biotin-succinimidyl ester (Molecular Probes) with O-(2-aminoethyl)-O′-(2-azidoethyl)-pentaethylene glycol (Fluka) in dry DMSO according to the manufacturer's instructions.

To synthesize propargyl-Cho, 4 g propargyl-bromide (80% solution in toluene, 34 mmol) were slowly added to 3 g dimethyl-ethanolamine (34 mmol) in 10 mL dry THF, while stirring on ice. The mix was allowed to reach room temperature and stirring was continued overnight. The resulting white solid was filtered and washed extensively with cold THF (10 × 20 mL), to afford pure propargyl-Cho bromide (5.9 g, 84% yield) as a white solid. Propargyl-Cho: white crystals, molecular weight: 128.19, ES-API LC/MS: $[M]^+ = 128.1$, ^{1}H NMR (600 MHz, CD_3OD): 4.78 (1H, b), 4.49 (2H, d, $J = 2.4$ Hz), 4.03 (2H, t, $J = 4.5$ Hz), 3.64 (2H, m), 3.30 (6H, s), ^{13}C NMR (600 MHz, CD_3OD): 83.2 (CH, d, $J = 101.4$ Hz), 72.7 (C, d, $J = 21.0$ Hz), 66.4 (CH_2, t, $J = 60.3$ Hz), 56.7 (CH_2, t, $J = 47.4$ Hz), 56.5 (CH_2, t, $J = 45.9$ Hz), 52.2 (C_2H_6, q, $J = 31.2$ Hz), 49.05 (CD_3OD).

ACKNOWLEDGMENTS. We thank Maria Ericsson for help with electron microscopy, Yao Chen for help with cryostat sections, Frank McKeon for help with mouse injections, Tom Kirchhausen (Harvard University, Cambridge, MA) for DNA constructs, and Tom Rapoport for helpful discussions. C.Y.J. is supported by an National Science Foundation fellowship. A.S. gratefully acknowledges the support from the Rita Allen Foundation, the Beckman Foundation, the Harvard-Armenise Foundation, and the American Asthma Foundation. Lipid analysis was performed at the Kansas Lipidomics Research Center. Instrument acquisition and method development was supported by the National Science Foundation (EPS 0236913, MCB 0455318, DBI 0521587), Kansas Technology Enterprise Corporation, K-IDeA Networks of Biomedical Research Excellence (INBRE) of National Institute of Health (P20RR16475), and Kansas State University.

1. Vance JE, Vance DE (2004) Phospholipid biosynthesis in mammalian cells. *Biochem Cell Biol* 82:113–128.
2. Nagan N, Zoeller RA (2001) Plasmalogens: Biosynthesis and functions. *Prog Lipid Res* 40:199–229.
3. Weiss SB, Smith SW, Kennedy EP (1958) The enzymatic formation of lecithin from cytidine diphosphate choline and D-1,2-diglyceride. *J Biol Chem* 231:53–64.
4. Rostovtsev VV, Green LG, Fokin VV, Sharpless KB (2002) A stepwise huisgen cycloaddition process: Copper(I)-catalyzed regioselective ''ligation'' of azides and terminal alkynes. *Angew Chem Int Ed Engl* 41:2596–2599.
5. Tornoe CW, Christensen C, Meldal M (2002) Peptidotriazoles on solid phase: [1,2,3]-triazoles by regiospecific copper (i) -catalyzed 1,3-dipolar cycloadditions of terminal alkynes to azides. *J Org Chem* 67:3057–3064.
6. Saxon E, Bertozzi CR (2000) Cell surface engineering by a modified Staudinger reaction. *Science* 287:2007–2010.
7. Vocadlo DJ, Hang HC, Kim EJ, Hanover JA, Bertozzi CR (2003) A chemical approach for identifying O-GlcNAc-modified proteins in cells. *Proc Natl Acad Sci USA* 100:9116–9121.
8. Beatty KE, et al. (2006) Fluorescence visualization of newly synthesized proteins in mammalian cells. *Angew Chem Int Ed Engl* 45:7364–7367.
9. Kiick KL, Saxon E, Tirrell DA, Bertozzi CR (2002) Incorporation of azides into recombinant proteins for chemoselective modification by the Staudinger ligation. *Proc Natl Acad Sci USA* 99:19–24.
10. Salic A, Mitchison TJ (2008) A chemical method for fast and sensitive detection of DNA synthesis in vivo. *Proc Natl Acad Sci USA* 105:2415–2420.
11. Jao CY, Salic A (2008) Exploring RNA transcription and turnover in vivo by using click chemistry. *Proc Natl Acad Sci USA* 105:15779–15784.
12. Bieber LL, Newburgh RW (1963) The incorporation of dimethylaminoethanol and dimethylaminoisopropyl alcohol into *Phormia regina* phospholipids. *J Lipid Res* 4:397–401.
13. Hodgson E, Dauterman WC (1964) The nutrition of choline, carnitine, and related compounds in the blowfly, *Phormia regina* Meigen. *J Insect Physiol* 10:1005–1008.
14. Bridges RG, Ricketts J (1970) The incorporation of analogues of choline into the phospholipids of the larva of the housefly, *Musca domestica*. *J Insect Physiol* 16:579–593.
15. Pasternak CA, Friedrichs B (1970) Turnover of mammalian phospholipids. *Biochem J* 119:481–488.
16. Macara IG (1989) Elevated phosphocholine concentration in ras-transformed NIH 3T3 cells arises from increased choline kinase activity, not from phosphatidylcholine breakdown. *Mol Cell Biol* 9:325–328.
17. Griffiths G (1993) in *Fine Structure Immunocytochemistry* (Springer Verlag, Heidelberg), p 459.
18. Stith BJ, et al. (2000) Quantification of major classes of *Xenopus* phospholipids by high performance liquid chromatography with evaporative light scattering detection. *J Lipid Res* 41:1448–1454.
19. Bartz R, et al. (2007) Lipidomics reveals that adiposomes store ether lipids and mediate phospholipid traffic. *J Lipid Res* 48:837–847.
20. Devaiah SP, et al. (2006) Quantitative profiling of polar glycerolipid species from organs of wild-type Arabidopsis and a phospholipase Dalpha1 knockout mutant. *Phytochemistry* 67:1907–1924.
21. Welti R, et al. (2002) Profiling membrane lipids in plant stress response. *J Biol Chem* 277:31994–32002.